All-Optical Comparator With a Step-Like Transfer Function

Li, Pu; Sang, Luxiao; Zhao, Dongliang; Fan, Yuanlong; Shore, K. Alan; Wang, Yuncai; Wang, Anbang

Journal of Lightwave Technology

DOI:
10.1109/JLT.2017.2766673

Published: 01/12/2017

Peer reviewed version

All-optical comparator with a step-like transfer function

Pu Li, Luxiao Sang, Dongliang Zhao, Yuanlong Fan, K. Alan Shore, *Senior Member, IEEE, Fellow, OSA*, Yuncai Wang, and Anbang Wang, *Member, IEEE*

***Abstract*—We propose a scheme for an all-optical comparator which embeds a nonlinear fiber ring resonator in a Mach-Zehnder configuration. Such a resonator accumulates the circulating power of the light traversing the ring, so that the effective nonlinear phase shift in fiber can be significantly enhanced. Numerical results demonstrate that with appropriate choice of the parameters of the Mach-Zehnder configuration and the power of the probe light, the all-optical comparator can exhibit an excellent step-like transfer function. Simultaneously the configuration reduces the switching threshold by 3 or more orders of magnitude to the level of mW when conventional highly nonlinear fibers are adopted. In addition, our simulations show that this all-optical threshold comparator also has a multi-periodic transfer characteristic and thus may be used to construct multi-bit analog-to-digital convertors.**

***Index Terms*—All-optical analog-to-digital conversion (ADC), all-optical signal processing, optical interferometry.**

I. Introduction

Since the 1970s, all-optical analog-to-digital conversion (AO-ADC) has been studied to overcome the conversion rate barrier arising with the electrical ADC.

The ADC consists of three basic functions: sampling, quantizing and coding. Much work has been undertaken in respect of the first two of those AO-ADC functions [1-2]. For instance, ultrafast optical sampling with a low jitter level of fetomseconds (fs) has become a reality because of the adoption of mode-locked laser pulse sources [3]. On the other hand, various optical solutions also have been proposed and demonstrated to improve the quantization performance by means of nonlinear optical phenomena such as optical amplitude or phase modulation [4-19-20-21], soliton splitting [22], supercontinuum generation [23], and self-frequency shift [24-26].

However, very few schemes have so far been proposed for the coding function of AO-ADC. For this third function of an AO-ADC, an all-optical comparator with a step-like response is the key to encode a finite number of different levels from the quantizing procedure into two distinct levels (either 0 or 1). Until now, nearly all of the reported results on optical ADC rely on electrical comparators to carry out this final threshold decision. The bandwidth bottleneck of electronic comparators drastically limits the performance of optical ADC. In 2013, Y. Ehrlichman *et al.* presented a *photonic* comparator, but their method still only accepts an electronic signal as the input [27]. Recently, we proposed an all-optical comparator based on optical hysteresis in a specially designed DFB semiconductor laser [28], yet its proved response rate is limited to 2.5 GHz by the slow recovery time of the semiconductor carrier distribution.

To realize coding function operation rates greater than that of electronic devices, the Kerr effect in highly nonlinear fiber (HNLF) is a promising approach. This is because the response time of the Kerr effect in fiber is a few fs (corresponding to a few hundred THz bandwidth), and it can induce various optical intensity-dependent phenomena such as self-phase modulation (SPM) and cross-phase modulation (XPM). Considering these advantages, K. Ikeda and his colleagues used a nonlinear optical loop mirror (NOLM) having the same function as an all-optical comparator [15-19]. However, the transfer function of the NOLM is sinusoidal, not step-like. Moreover, because conventional HNLFs possess a typical nonlinear coefficient γ between 10 $W^{-1}Km^{-1}$ and 20 $W^{-1}Km^{-1}$, a high incident power with a typical level of W is needed to achieve the desired effect.

In this paper, we propose and analyze an all-optical comparator using a nonlinear fiber ring resonator (NFRR) embedded in a Mach-Zehnder interferometer (MZI). Our simulations show that the introduction of the fiber resonator can effectively accumulate the nonlinear phase shift and thereby ensure that the associated transfer function has ideal step-like transfer characteristics. At the same time, the switching threshold power is also greatly reduced to of order mW. In addition, we show that our all-optical comparator has the potential ability to be used for multi-bit AO-ADC, because of its multi-periodic square-wave transfer function.

This work was supported by National Natural Science Foundation of China (NSFC) under Grants 61505137, 61475111, and 61527819, U. K. Engineering and Physical Sciences Research Council (EPSRC) under Grant EP/P006027/1, National Cryptography Development Fund under Grant MMJJ20170127, Natural Science Foundation of Shanxi under Grant 2015021088, and Scientific and Technological Innovation Programs of Higher Education Institutions in Shanxi under Grant 2015122.

Pu Li, Luxiao Sang, Dongliang Zhao, Yuncai Wang, and Anbang Wang are with Key Laboratory of Advanced Transducers & Intelligent Control System, Ministry of Education, Taiyuan University of Technology, and Institute of Optoelectronic Engineering, College of Physics & Optoelectronics, Taiyuan University of Technology, Taiyuan, 030024 China (e-mail: lipu8603@126.com;sangluxiao@163.com;zhaodl633@163.com;wangyc@tyut.edu.cn; wanganbang@tyut.edu.cn).

Pu Li, Yuanlong Fan, and K. Alan Shore are with School of Electronic Engineering, Bangor University, Wales, LL57 1UT U. K. (e-mail: lipu8603@126.com; y.fan@bangor.ac.uk; k.a.shore@bangor.ac.uk).

II. Configuration and Theory Of All-optical Comparator Using NFFR-Embedded In MZI

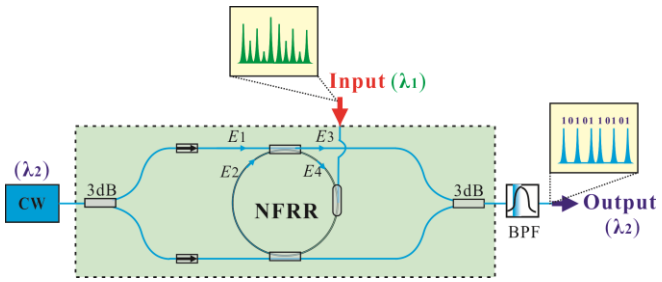

Fig. 1. Schematic of the proposed all optical comparator with a step-like transfer function. CW, continuous-wave probe light; 3dB, 3dB optical coupler; NFRR, nonlinear fiber ring resonator; BPF, optical band-pass filter; Input, the quantized pulse input to be coded at a wavelength of λ_1; Output, the coded output of the probe light at a wavelength of λ_2.

As depicted in the dashed box in Fig. 1, the proposed all-optical comparator has a configuration of a MZI with two arms sharing a NFRR. The optical pulses to be coded operate at a wavelength of λ_1 and are input into the NFRR as the control light via a wavelength division multiplexing (WDM) coupler. A continuous-wave light with a resonating wavelength of λ_2 (used as the probe light) is injected into the MZI through a 3 dB coupler and then split into two equal parts: one in the upper arm of the MZI is coupled into the NFRR and propagates in the clockwise direction, which is in the same direction with the control pulse light; the other in the lower arm of the MZI is coupled into the nonlinear fiber ring, but transmits in the counterclockwise direction. In this way, the two parts of the probe light will experience different nonlinear phase shifts in the NFRR due to the SPM and XPM. Finally, the interferometer output of probe light will be filtered out by an optical band-pass filter (BPF), which only passes the light with the same wavelength of λ_2.

Specifically, the coupling of the probe light in the upper arm into and out of the NFRR can be described in terms of the well-known field transfer characteristics [29, 30]:

$$E_3 = rE_1 + itE_2 \tag{1}$$

$$E_4 = itE_1 + rE_2 \tag{2}$$

$$E_2 = \eta e^{i\varphi} E_4 \tag{3}$$

, where r and t are the coupling parameters (satisfying the relation $r^2+t^2=1$). The fields of E_1, E_2, E_3 and E_4 are defined with respect to the reference points indicated in Fig. 1. φ represents the single-trip phase shift induced by the circumference l of the NRFF and η is the associated transmission factor.

The probe light is at the on-resonance transmission wavelength λ_2 [which satisfies $nl = m\lambda_2$, where n is the refractive index of nonlinear ring and m is a positive integer, respectively], so that the single-trip phase shift φ can be expressed as $\varphi = 2\pi nl/\lambda_2 = 2m\pi$. Solving Eqs.(1) - (3) simultaneously, we can find that E_3 and E_1 are related by the following complex amplitude transmission

$$\frac{E_3}{E_2} = \frac{r - \eta \exp(i\varphi)}{1 - \eta r \exp(i\varphi)} \tag{4}$$

Thus, the associated intensity transmission factor t can be given by the squared modulus

$$t = \left|\frac{E_3}{E_2}\right|^2 = \frac{\eta^2 + r^2 - 2\eta r\cos(\varphi)}{1 + \eta^2 r^2 - 2\eta r\cos(\varphi)} \tag{5}$$

Note that the on-resonance transmission drops to zero for the situation $r=\eta$, which is called as "critical coupling" [30]. In this case, the resonant depth can reach the maximum point and thus the circulating power of the light traversing the ring can get an optimal accumulation [29]. Therefore, the phase difference ϕ between E_3 and E_1 can be obtained by the argument of Eq. (4) as follow:

$$\phi = \frac{\pi}{2} - arctan\left(\frac{1+r^2}{1-r^2} tan\frac{\varphi}{2}\right) \tag{6}$$

Considering the XPM induced by the control pulse train, the XPM between the two parts of resonant probe light and the SPM of the probe light itself, we can finally obtain the efficient phase difference $\Delta\phi$ between the upper arm and the lower arm of MZI from Eq. (6):

$$\Delta\phi = arctan\left(\frac{1+r^2}{1-r^2} tan\frac{\varphi_1}{2}\right) - arctan\left(\frac{1+r^2}{1-r^2} tan\frac{\varphi_2}{2}\right) \tag{7}$$

, where φ_1 and φ_2 are the single-trip phase shift of the probe lights in the lower arm and upper arm, respectively. They can be written as follows:

$$\varphi_1 = 2\pi nl/\lambda_2 + 3\gamma lP_1 + 2\gamma lP_2 \tag{8}$$

$$\varphi_2 = 2\pi nl/\lambda_2 + 3\gamma lP_1 \tag{9}$$

Note, $2\pi nl/\lambda_2$ is the linear phase shift of the probe light, $3\gamma lP_1$ is the nonlinear phase shift introduced by SPM of the probe light itself, $2\gamma lP_2$ is the nonlinear phase shift introduced by XPM between control pulse and probe light. Here, γ is the nonlinear coefficient of nonlinear ring, P_1 is the power of probe light, and P_2 is the peak power of control pulse.

The transmission T of the probe light output from the BPF can be written as:

$$T = \frac{1 - cos\Delta\phi}{2} \tag{10}$$

When the peak power of the control pulse P_2 is low, the difference between φ_1 and φ_2 is very small. From Eqs. (7), (9) and (10), we can obtain that $T=0$. On the other hand, when the P_2 is large enough to obtain $\varphi_1 > 2\pi$, $tan(\varphi_1/2)$ will change from less than 0 to greater than 0 and thus $arctan[(1+r^2)/(1-r^2)tan(\varphi_1/2)]$ will appropriately equal $\pi/2$. Usually the XPM between counter-propagating probe light and control pulses can be ignored so that $arctan[(1+r^2)/(1-r^2)tan(\varphi_2/2)]$ is appropriately equivalent to $-\pi/2$. From Eqs. (7) and (9), it can then be obtained that $\Delta\phi=\pi$ and thus $T=1$.

III. Simulation Results

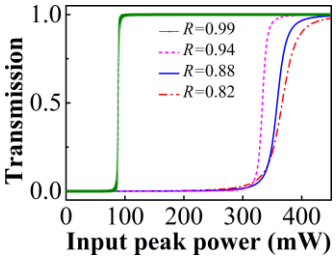

Fig. 2. Transfer functions of the all-optical comparators with different coupling ratios R.

Figure 2 shows some typical transfer functions of the proposed all-optical comparator with respect to input pulse peak power at different coupling ratio $R=r^2$. It must be noted that the input optical power in Fig. 2 is the peak power of the control pulse, not the average power as in Refs. [15-19]. In our simulation, the wavelength (λ_2) of control pulse is fixed at 1554 nm with a 10 GHz repetition frequency and a 14 ps pulse width, and the CW probe light is operating at the wavelength (λ_1) 1550 nm. The other parameters are fixed at typical practical values as follows: l = 200 m, γ= 20 $W^{-1}Km^{-1}$ and P_1 = 2.0 mW. From Fig. 2, it is clear that all the slopes of the transfer functions exhibit a steep curve for all the coupling coefficients. The phase difference $\Delta\phi$ depends sensitively on the coupling coefficient r. In Fig. 2, the transfer curve is seen to approach a step-like shape with the coupling ratio R increasing from 0.82 to 0.99. On the other hand, one can observe that the threshold power will rapidly decrease from more than 300 mW to less than 100 mW, when the coupling coefficient approaches unity. All of these curves demonstrate that the phase difference $\Delta\phi$ may indeed become greatly enhanced due to the effective accumulation of the nonlinear phase shift by the NFRR.

Next, we investigate the influence of some other critical parameters on the transfer function of the all-optical comparator. These parameters include the nonlinear coefficient (γ) of the HNLF, the circumference (l) of the NFRR and the power of the probe light (P_1). Figure 3 shows the effect of the nonlinear coefficient (γ) on the transfer function of the proposed all-optical comparator, where l = 200 m, R = 0.99 and P_1 = 2.0 mW. From Fig. 3, it can be seen that, with increase of the HNLF nonlinear coefficient γ, the threshold value of the all-optical comparator greatly decreases, but the slope of the transfer curve does not change very much. Similar to the effect of the nonlinear coefficient γ, it is observed from Fig. 4 that an increase of the NFRR circumference (l) will greatly reduce the threshold of the transfer curve while its slope only becomes a little steeper. This means that if we only want a step-like transfer function, the fiber length l can be reduced further to the level of several m. In this current scenario, P_1=2.0 mW, R=0.99 and γ= 20 $W^{-1}Km^{-1}$. The reason for Figs. 3 and 4 can be simply explained from Eqs. (6) and (7): the induced nonlinear phase-shift is proportional to both the nonlinear coefficient (γ) and the circumference (l) of the NFRR.

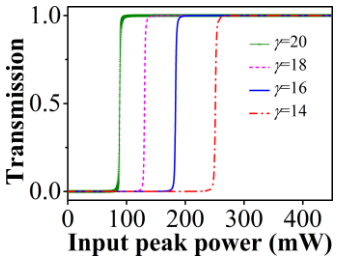

Fig. 3. Influence of the nonlinear coefficient (γ) on the transfer function for the all-optical comparator, where l = 200 m, R = 0.99 and P_1 = 2.0 mW.

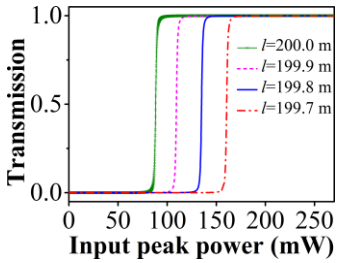

Fig. 4. Influence of the nonlinear fiber length (l) on the transfer function for the all-optical comparator, where P_1=2.0 mW, R=0.99 and γ= 20 $W^{-1}Km^{-1}$.

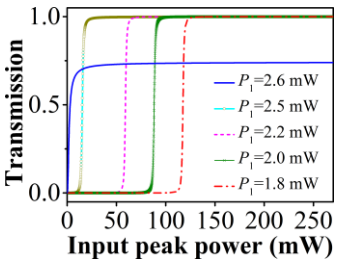

Fig. 5. Influence of the probe power (P_1) on the transfer function for the all-optical comparator, where l = 200 m, R = 0.99 and γ= 20 $W^{-1}Km^{-1}$.

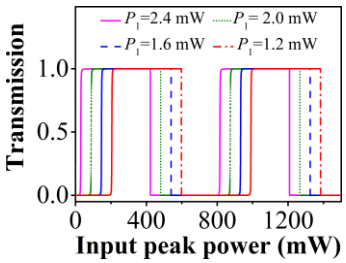

Fig. 6. Multi-period transfer functions of the all-optical comparators with different probe power P_1, where l=200 m, R=0.99, and γ= 20 $W^{-1}Km^{-1}$.

Figure 5 depicts the influence of the probe power on the transfer function, where l = 200 m, R = 0.99 and γ= 20 $W^{-1}Km^{-1}$. From Fig. 5, we notice that the switching threshold can be further reduced when the power of the probe light is enhanced. This is because increasing the probe light power will enhance the SPM effect, which corresponds to the term '$3\gamma lP_1$' in Eqs. (6) and (7). However, it should be pointed out that once the power is higher than some value - as with the transfer curve in Fig. 5 corresponding to P_1 = 2.6 mW - the 100% transmission cannot be maintained. This indicates that there is a tradeoff between the optimized threshold and transmission. Careful

choice should be made of the probe light power when a lower threshold is sought.

Further, by increasing the input power range, we find that the proposed all-optical comparator can exhibit a square-wave-like multi-period transfer function. This is demonstrated in Fig. 6, which illustrates the transfer functions with respect to the input peak power of control pulse for different probe light power [P_1= 2.4 mW, 2.0 mW, 1.6 mW or 1.2 mW]. The other parameters in this simulation are set as follows: l=200 m, R=0.99, and γ= 20 W^{-1}Km^{-1}. Moreover, it should also be noticed that by controlling the power of probe light P_1 one can easily shift the onset of the multi-period optical transfer function.

The above multi-period characteristic enables our proposed all-optical comparator to be extended to realize multi-bit AO-ADC. For an m-bit AO-ADC, an array of m comparators with different-period transfer functions are needed. The input optical pulse sampled from an analog signal are split into m identical optical pulse streams, and then launched into the parallel array of m comparators, respectively. Each comparator has a different-period transfer function with respect to the input optical pulses, so that every input pulse can be simultaneously converted into an m-bit parallel digital binary signal. For conciseness, we take a 3-bit ADC (i.e., m=3) as an example. As shown in Fig. 7(a), three all-optical comparators [denoted as i, ii and iii] process half-, single- and two-period transfer functions, respectively. Note, the NFRR lengths of the three comparators from top to bottom are 200 m, 200.4 m and 400.7 m, while the associated probe powers are 10.6 mW, 11.868 mW and 8.016 mW, respectively. The other parameters are the same as that in Fig. 6. By these means, the whole input pulse power scope can be Gray-coded into to 8 quantization levels according to the different parallel output of the comparator array (#i #ii #iii). Figure 7(b) is the obtained Gray code output versus the input pulse peak power in the simulation, which are **100**, **101**, **111**, **110**, **010**, **011**, **001** and **000**, respectively.

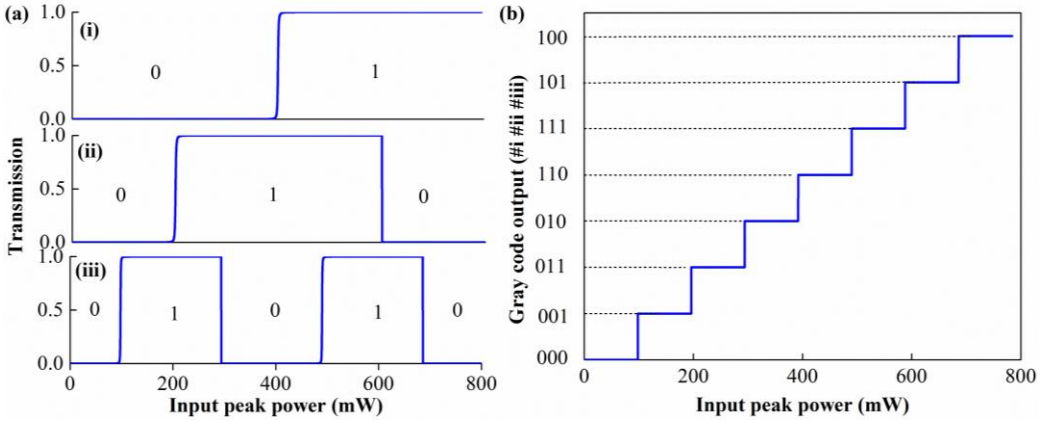

Fig. 7. (a) Transfer functions of the three all-optical comparators [denoted as (i), (ii) and (iii)] for the realization of a 3-bit ADC and (b) Gray code output versus the input peak power in the simulation of 3-bit AO-ADC. Herein, the NFRR lengths of the three comparators [denoted as (i), (ii) and (iii) in Fig. 7(a)] are 200 m, 200.4 m and 400.7 m, while the associated probe powers are 10.6 mW, 11.868 mW and 8.016 mW, respectively. The other parameters are the same as that in Fig. 6.

IV. Discussion

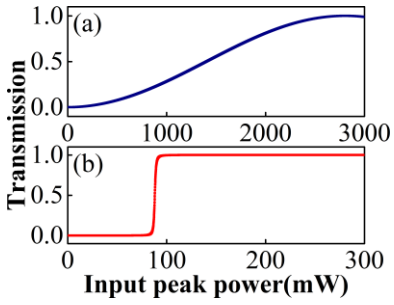

Fig. 8. Transfer functions of (a) a standard NOLM with l=200 m and γ= 20 W^{-1}Km^{-1} and (b) the all-optical comparators with l=200 m, γ= 20 W^{-1}Km^{-1}, R=0.99, and P_1=2.0 mW.

Firstly, we want to discuss the benefits of the proposed all-optical comparator scheme by making a direct comparison between the transfer functions for a standard MZI and our NFRR-based MZI with the same 200 m length of HNLF. The standard MZI is a MZI with an unbalanced length of HNLF in the upper arm, where the input optical pulse as the control light is coupled via a WDM coupler. As pointed out in Ref. [17], this standard MZI is equivalent to the NOLM in the simulation. Figure 8(a) shows the simulated transfer function of the standard MZI, which is consistent with the experimental and numerical results in Ref. [17]. From it, one can clearly observe that the transmission rates continuously vary with increase of the input pulse power and thus no distinct threshold exists. In comparison, the transfer function of our proposed NFRR-introduced MZI under the same condition is shown in Fig. 8(b). Due to the enhanced nonlinearity by the NFRR, our nonlinear MZI exhibits a step-like transfer function with a distinct threshold less than 100 mW. Moreover, it can be seen by comparing Figs. 8(a) and 8(b) that the requirements for the input pulse power are greatly reduced. It should be pointed out that the probe light power (P_1) in Fig. 8(b) is 2.0 mW. When P_1 less than 2.5 mW is used, the input threshold power can be further reduced into several mW, as shown in Fig. 5. This means that except for the step-like transfer function, our proposed MZI configuration (*i.e.*, all-optical comparator) can simultaneously reduce the switching threshold by 3 orders of magnitude to the level of mW, even though the conventional HNLF is adopted.

Secondly, we discuss the effect of the neglected losses in the above simulations (*i.e.*, the fiber loss and the insert loss induced the WDM

coupler) on the transfer function of the proposed all-optical comparator. For this purpose, three scenarios are considered: (i) the loss is neglected as the previous sections; (ii) only the fiber loss is considered with a typical attenuation coefficient of 0.5 dB/km; (iii) both the fiber loss and the WDM insertion loss are considered, where the insertion loss is typically 1 dB. In the simulation, Eq. (6) is replaced by the following:

$$\begin{aligned}\phi &= \arg\left(\frac{r - rae^{-j\varphi}}{1 - r^2 ae^{-j\varphi}}\right) \\ &= \frac{\pi}{2} - arctan\left(\frac{-a(1+r^2)\cos\varphi + 1 + r^2a^2}{(1-r^2)a\sin\varphi}\right)\end{aligned} \tag{11}$$

Here, $a = \sqrt{(1-\beta)\exp(-\alpha l)}$, is termed the loss rate of the NFRR, where β and α represent the insert loss of the WDM coupler and the attenuation coefficient of the fiber, respectively. Figure 9 shows the three associated simulated transfer functions. It can be seen clearly that the losses have no significant influence on the step-like characteristic of the transfer function. With increase of the losses, the threshold value of the all-optical comparator slightly increases. However, it should be pointed that the increased threshold is still at a relatively low level compared to that in a NOLM. Moreover, if the power of the probe light is appropriately increase, a lower threshold of several mW can be expected as shown in Fig. 5.

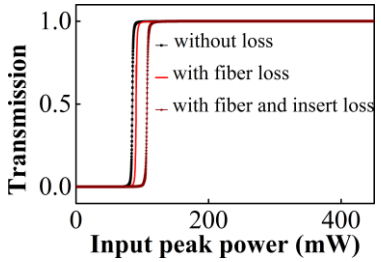

Fig. 9. Transfer functions of the all-optical comparators with different losses, where l=200 m, γ= 20 W^{-1}Km^{-1}, R=0.99, and P_1=2.0 mW.

In addition, we want to point out that in our simulation the control and probe light are assumed to maintain the same polarization state. Due to the birefringence of conventional highly nonlinear fiber (HNLF), the NFRR (nonlinear fiber ring resonator) will suffer from a polarization state mismatch between control pulse and probe light and that may cause the transfer function to be distorted unpredictably or non-periodically [31-32]. Therefore, the control and probe light are assumed to maintain the same polarization state in our proposal. This can be realized in practical implementation by two techniques: (i) the simplest method is to use a polarization-maintaining HNLF for the NFRR, as done in Ref. [18-19]; (ii) if a non-polarization-maintaining HNLF is used to construct the NFRR, the polarization matching condition can be obtained by means of polarization control techniques [15-17].

V. Conclusions

In conclusion, we have proposed a novel all-optical comparator using a NFRR-based MZI for the coding function of AO-ADC. Numerical results demonstrate that a step-like transfer function with a low threshold power can be obtained due to the effective enhancement of the accumulated nonlinear phase shift by the introduction of NFRR. The shape and threshold of the step-like transfer depends on three critical parameters of the nonlinear MZI and on the power of the probe light. Further simulations show that the proposed all-optical threshold comparator can exhibit rectangular multi-period transfer characteristics and thus has the potential to act as a multi-bit AO-ADC.

References

[1] G. C.Valley, "Photonic analog-to-digital converters," *Opt. Express*, vol.15, no. 5, pp. 1955-1982, Mar. 2007.

[2] Z. Zhang, H. Li, S. Zhang, and Y. Liu, "Analog-to-digital converters using photonic technology," *Chin. Sci. Bull.*, vol. 59, no. 22, pp. 2666-2671, May 2014.

[3] A. Khilo, S. J. Spector, M. E. Grein, A. H. Nejadmalayeri, C. W. Holzwarth, M. Y. Sander, M. S. Dahlem, M. Y. Peng, M. W. Geis, N. A. DiLello, J. U. Yoon, A. Motamedi, J. S. Orcutt, J. P. Wang, C. M. Sorace-Agaskar, M. A. Popović, J. Sun, G.-R. Zhou, H. Byun, J. Chen, J. L. Hoyt, H. I. Smith, R. J. Ram, M. Perrott, T. M. Lyszczarz, E. P. Ippen, and F. X. Kärtner, "Photonic ADC: overcoming the bottleneck of electronic jitter," *Opt. Express*, vol. 20, no. 4, pp. 4454-4469, Feb. 2012.

[4] H. Taylor, "An optical analog-to-digital converter—Design and analysis," *IEEE J. Quantum Electron.*, vol. 15, no. 4, pp. 210–216, Apr. 1979.

[5] J. Stigwall and S. Galt, "Interferometric analog-to-digital conversion scheme," *IEEE Photon. Technol. Lett.*, vol. 17, no. 2, pp. 468–470, Feb. 2005.

[6] J. Stigwall and S. Galt, "Demonstration and analysis of a 40-Gigasample/s interferometric analog-to-digital converter," *J. Lightw. Technol.*, vol. 24, no. 3, pp. 1247–1256, Mar. 2006.

[7] H. Chi and J. Yao, "A photonic analog-to-digital conversion scheme using Mach-Zehnder modulators with identical half-wave voltages," *Opt. Express*, vol. 16, no. 2, pp.567-572, Jan. 2008.

[8] Q. Wu, H. Zhang, M. Yao, and W. Zhou, "All-optical analog-to-digital conversion using inherent multiwavelength phase shift in LiNbO3 phase modulator," *IEEE Photon. Technol. Lett.*, vol. 20, no. 12, pp. 1036–1038, Jun. 2008.

[9] Y. Peng, H. Zhang, Q. Wu, X. Fu, and M. Yao, "Adaptive thresholding scheme in photonic analog-to-digital conversion," *Opt. Lett.*, vol. 34, no. 14, pp. 2201-2203, Jul. 2009.

[10] Y. Peng, H. Zhang, Q. Wu, Y. Zhang, X. Fu, and M. Yao, "Experimental demonstration of all-optical analog-to-digital conversion with balanced detection threshold scheme," *IEEE Photon. Technol. Lett.*, vol. 21, no. 23, pp.1776-1778, Dec. 2009.

[11] C. H. Sarantos and N. Dagli, "A photonic analog-to-digital converter based on an unbalanced Mach-Zehnder quantizer," *Opt. Express*, vol. 18, no. 14, pp. 14598-14603, Jul. 2010.

[12] S. Wei, J. Wu, L. Zhao, C. Yao, J. Chen, D. Lu, X. Zhang, and Z. Yin, "Multimode interference coupler based photonic analog-to-digital conversion scheme," *Opt. Lett.*, vol. 28, no. 12, pp. 3699-3701, Sep. 2012.

[13] Z. Kang, X. Zhang, J. Yuan, X. Sang, Q. Wu, G. Farrell, and C. Yu, "Resolution-enhanced all-optical analog-to-digital converter employing cascade optical quantization operation," *Opt. Express*, vol. 22, no. 18, pp. 21441-21453, Sep. 2014.

[14] D. Peng, Z. Zhang, Y. Ma, Y. Zhang, S. Zhang, and Y. Liu, "Broadband linearization in photonic time-stretch analog-to-digital converters employing an asymmetrical dual-parallel Mach-Zehnder modulator and a balanced detector," *Opt. Express*, vol. 24, no. 11, pp. 11546-11557, May 2016.

[15] K. Ikeda, J. M. Abdul, S. Namiki, and K. Kitayama, "Optical quantizing and coding for ultrafast A/D conversion using nonlinear fiber-optic switches based on Sagnac interferometer," *Opt. Express*, vol. 13, no. 11, pp. 4296-4302, May 2005.

[16] K. Ikeda, J. M. Abdul, H. Tobioka, T. Inoue, S. Namiki, and K. Kitayama, "Design considerations of all-optical A/D conversion: nonlinear fiber-optic sagnac-loop interferometer-based optical

quantizing and coding," *J. Lightw. Technol.*, vol. 24, no. 7, pp. 2618-2628, Jul. 2006.

[17] Y. Miyoshi, K. Ikeda, H. Tobioka, T. Inoue, S. Namiki, and K. Kitayama, "All-optical analog-to-digital conversion using split-and-delay technique," *J. Lightw. Technol.*, vol. 25, no. 6, pp. 1339-1347, Jun. 2007.

[18] Y. Miyoshi, S. Takagi, S. Namiki, and K. Kitayama, "Multiperiod PM-NOLM with dynamic counter-propagating effects compensation for 5-bit all-optical analog-to-digital conversion and its performance evaluations," *J. Lightw. Technol.*, vol. 28, no. 4, pp.415-422, Feb. 2010.

[19] Y. Miyoshi, S. Namiki, and K. Kitayama, "Performance evaluation of resolution-enhanced ADC using optical multiperiod transfer functions of NOLMs," *IEEE J. Sel. Topics Quantum Electron.*, vol.18, no. 2, pp.779-784, Mar./Apr. 2012.

[20] Z. Kang, J. Yuan, X. Zhang, X. Sang, K. Wang, Q. Wu, B. Yan, F. Li, X. Zhou, K. Zhong, G. Zhou, C. Yu, G. Farrell, C. Lu, H. Tam, and P. Wai, "On-chip integratable all-optical quantizer using strong cross-phase modulation in a silicon-organic hybrid slot waveguide," *Sci. Rep.*, vol. 6, pp.19528, 2016.

[21] Z. Kang, J. Yuan, X. Zhang, Q. Wu, X. Sang, G. Farrell, C. Yu, F. Li, H. Tam, and P. Wai, "CMOS-compatible 2-bit optical spectral quantization scheme using a silicon-nanocrystal-based horizontal slot waveguide," *Sci. Rep.*, vol. 4, pp.7177, 2014.

[22] S. Oda, A. Maruta, and K. Kitayama, "All-optical quantization scheme based on fiber nonlinearity," *IEEE Photon. Technol. Lett.*, vol. 16, no. 2, pp. 587–589, Feb. 2004.

[23] S. Oda and A. Maruta, "A novel quantization scheme by slicing supercontinuum spectrum for all-optical analog-to-digital conversion," *IEEE Photon. Technol. Lett.*, vol. 17, no. 2, pp. 465–467, Feb. 2005.

[24] C. Xu and X. Liu, "Photonic analog-to-digital converter using soliton self-frequency shift and interleaving spectral filters," *Opt. Lett.*, vol. 28, no. 12, pp. 986–988, Jun. 2003.

[25] T. Nishitani, T. Konishi, and K. Itoh, "Optical coding scheme using optical interconnection for high sampling rate and high resolution photonic analog-to-digital conversion," *Opt. Express*, vol. 15, no. 24, pp. 15812-15817, Nov. 2007.

[26] Z. Kang, J. Yuan, Q. Wu, T. Wang, S. Li, X. Sang, C. Yu, and G. Farrell, "Lumped time-delay compensation scheme for coding synchronization in the nonlinear spectral quantization-based all-optical analog-to-digital conversion," *IEEE Photon. J.*, vol. 5, no. 6, p. 7201109, Dec. 2013.

[27] Y. Ehrlichman, O. Amrani, and S. Ruschin, "Integrated photonic threshold comparator based on square-wave synthesis," *Opt. Express*, vol. 21, no. 12, pp. 14251-14261, Jun. 2013.

[28] P. Li, X. Yi, X. Liu, D. Zhao, Y. Zhao, and Y. Wang, "All-optical analog comparator," *Sci. Rep.*, vol. 6, p. 31903, Aug. 2016.

[29] J. E. Heebner, V. Wong, A. Schweinsberg, R. W. Boyd, and D. J. Jackson, "Optical transmission characteristics of fiber ring resonators," *IEEE J. Quantum Electron.*, vol. 40, no. 6, pp.726–730, Jun. 2004.

[30] A. Yariv, "Critical coupling and its control in optical waveguide-ring resonator systems," *IEEE Photon. Technol. Lett.*, vol. 14, no. 4, pp. 483-485, Apr. 2002.

[31] Y. Miyoshi, S. Takagi, H. Nagaeda, S. Namiki, and K. Kitayama, "Toward tera-sample/s 5-bit all-optical analog-to-digital conversion," in *Proc. Optical Fiber Communication Conf. Expo. (OFC 2009)*, OMI 4, Mar. 2009.

[32] Y. Miyoshi, S. Takagi , H Nagaeda, N Shu, and K. Kitayama, "Ultrafast all-optical A/D conversion using NOLMs with multiperiod transfer functions," in *Proc. LEOS Winter Topicals 2009*, TuC. 1.2., Jan. 2009.

Pu Li received the M. S. degree in physical electronics from Taiyuan University of Technology (TYUT), Shanxi, China, in 2011. In 2014, he received the Ph. D. degree in circuits and systems at the Key Laboratory of Advanced Transducers and Intelligent Control System (Ministry of Education of China), College of Physics and Optoelectronics, TYUT, Shanxi, China.

In 2014, He joined TYUT. Currently, he is an assistant professor at the College of Physics and Optoelectronics, TYUT. Meanwhile, he is a Visiting Scholar at the School of Electronic Engineering, Bangor University, United Kingdom. His research interests include all-optical analog-to-digital conversion, all-optical signal processing, fiber nonlinear optics, nonlinear dynamics of semiconductor lasers and its applications.

Dr. Li is a Member of the Chinese Optical Society and the Chinese Physical Society. He also serves as a reviewer for journals of the OSA and Elsevier organizations.

Luxiao Sang received the M. S. degree in optical engineering from Taiyuan University of Technology (TYUT), Shanxi, China, in 2017. He is currently working towards Ph. D. degree at the Key Laboratory of Advanced Transducers and Intelligent Control System (Ministry of Education of China), TYUT, Shanxi, China.

His research interests focus on all-optical analog-to-digital conversion.

Dongliang Zhao received the M. S. degree in physical electronics from Taiyuan University of Technology (TYUT), Shanxi, China, in 2017. He is currently working towards Ph. D. degree at the Key Laboratory of Advanced Transducers and Intelligent Control System (Ministry of Education of China), TYUT, Shanxi, China.

His research interests focus on all-optical analog-to-digital conversion.

Yuanlong Fan received the B. E. degree from Dalian University of Technology, China, in 2009 and his M.E. and Ph.D. degrees from the University of Wollongong, Australia, in 2011 and 2016, respectively, all in electronic engineering. He was a recipient of the Australian Endeavour Fellowship to undertake postdoctoral research at the University of Wollongong, Australia in 2016.

He is currently a research officer at the School of Electronic Engineering, Bangor University, United Kingdom. His research interests include nonlinear dynamics of semiconductor lasers, fiber nonlinear optics, and optical signal processing.

K. Alan Shore (SM'95) received the degree in mathematics from the University of Oxford, Oxford, U.K., and the Ph.D. degree from University College, Cardiff, Wales, U. K.

He was a Lecturer with the University of Liverpool from 1979 to 1983 and with the University of Bath, where he became a Senior Lecturer in 1986, a Reader in 1990, and a Professor in 1995. He was a Visiting Researcher with the Center for High Technology Materials, University of New Mexico, Albuquerque, USA, in 1987. In 1989, he was a Visiting Researcher with the Huygens Laboratory, Leiden University, The Netherlands. From 1990 to 1991, he was with the Teledanmark Research Laboratory and the MIDIT Center of the Technical University of Denmark, Lyngby. He was a Guest Researcher with the Electrotechnical Laboratory, Tsukuba, Japan, in 1991. In 1992, he was a Visiting Professor with the Department of Physics, University de les IllesBalears, Palma–Majorca, Spain. He was a Visiting Lecturer with the Instituto de Fisica de Cantabria, Santander, Spain, from 1996 to 1998, and a Visiting Researcher with the Department of Physics, Macquarie University, Sydney, Australia, in 1996, 1998, 2000, 2002, 2005, and 2008. In 2001, he was a Visiting Researcher with the ATR Adaptive Communications Laboratories, Kyoto, Japan. From 2001 to 2008, he was the Director of Industrial and Commercial Optoelectronics, a Welsh Development Agency Center of Excellence. Since 1995, he has been the Head of the School of Informatics, College of Physical and Applied Sciences, Bangor University. He has authored or co-authored more than 1000 contributions to archival journals, books, and technical conferences. With Prof. D. Kane, he co-edited the research monograph Unlocking Dynamical Diversity. His research work has been principally in the area of semiconductor optoelectronic device design and experimental characterization with particular emphasis on nonlinearities in laser diodes and semiconductor optical waveguides. His current research interests include nonlinear optics and its applications, and the design of nano-spin semiconductor lasers. In 1995, he was appointed as the Chair of Electronic Engineering with Bangor University. He was the Chair of the Welsh Optoelectronics Forum from 2006 to 2008 and has chaired the Photonics Academy for Wales, since its establishment in 2005. From 2008 to 2011, he was the Chair of the Quantum Electronics Commission of the International Union of Pure and Applied Physics.

Dr. Shore has been a Program Member for several OSA conferences. He was a Co-Organizer of a Rank Prize Symposium on Nonliear Dynamics in Lasers held at the lake district, U.K., in 2002. He cofounded and from 1987 to 2012 acted as the Organizer and Program Committee Chair for the International Conference on Semiconductor and Integrated Optoelectronics, which is held annually in Cardiff, Wales, U.K. He chaired the Education and Training in Optics and Photonics conference held at the Technium OpTIC, Wales, 2009. He received the Royal Society Travel Grant to visit universities and laboratories in Japan in 1988. From July to December 2010, he held a Japan Society for the Promotion of Science Invitation Fellowship in the Ultrafast Photonics Group, Graduate School of Materials Science, Nara Institute of Science and Technology, Nara, Japan. He is a Fellow of the Optical Society of America, the Institute of Physics, and the Learned Society of Wales for which

he has served as a Council Member (2012-2015; 2016-2019) and General Secretary (2017-2020).

Yun-cai Wang was born in Shanxi, China. He received the B.S. degree in semiconductor physics from Nankai University, Tianjin, China, in 1986, and the M. S. and Ph. D. degrees in physics and optics from Xi'an Institute of Optics and Precision Mechanics of Chinese Academy of Sciences (CAS), Shaanxi, China, in 1994 and 1997, respectively.

In 1986, he joined TYUT, as a teaching assistant. He was a Visiting Scholar at the Institut für Festkörperphysik, Technische Universität Berlin, Berlin, Germany, from 2001 to 2002. He was a Lecture (1994-1998) and then an Assistant Professor (1998-2003) at the Department of Physics, TYUT. Since 2003, he has been a Professor at the College of Physics and Optoelectronics, TYUT. Now, he also is the chair of the Key Laboratory of Advanced Transducers and Intelligent Control System (Ministry of Education of China). His current research interests are nonlinear dynamics of semiconductor lasers and fibers and their applications, including all-optical analog-to-digital conversion, and optical communications.

Dr. Wang is a Fellow of the Chinese Instrument and Control Society, a Senior Member of the Chinese Optical Society and the Chinese Physical Society. He also serves as a reviewer for journals of the IEEE, OSA and Elsevier organizations.

An-bang Wang received the M. S. degrees in physical electronics and the Ph. D degree in electronic circuit and system from TYUT in 2006 and 2014, respectively.

He joined TYUT as a lecture in 2006 and became a professor in 2015 at the College of Physics and Optoelectronics, TYUT. Between Dec. 2014 and May 2015, he was a visiting scholar with the School of Electronic Engineering, Bangor University, U.K. His research interests include nonlinear dynamics of semiconductor lasers and its applications, all-optical analog-to-digital conversion, optical signal processing, fiber nonlinear optics and optical communications.

Dr. Wang is a Member of the IEEE Society. He is a committee member of Opto-Electronic Technology Professional Committee, the Chinese Optical Society. He serves as a topical editor of Acta Optica Sinica, and as a reviewer for journals of the IEEE and OSA organizations.